

Sharina M.E.* and Maricheva M.I.

Chemical composition and ages of four globular clusters in M31 from the analysis of their integrated-light spectra

DOI: DOI

Received ..; revised ..; accepted ..

Abstract: We compare the results on the chemical composition of four globular clusters (GCs) in M31 (Bol6, Bol20, Bol45, and Bol50) (Maricheva 2021. Study of integrated spectra of four globular clusters in M 31. *Astrophys. Bull.* 76:389–404. doi: <https://doi.org/10.1134/S199034132104009X>) to the available literature data on integrated-light spectroscopy of globular clusters with similar ages and chemical abundances in our Galaxy and M31 and on the chemical abundances of stars in two galaxies. The clusters and their literature analogues are of moderate metallicity $-1.1 < [\text{Fe}/\text{H}] < -0.75$ dex and older (10 Gyr). Mg, Ca, and C abundances of four GCs are higher than literature estimates for the GCs in M31 with $[\text{Fe}/\text{H}] \sim -1$ dex obtained using high-resolution integrated-light spectroscopy methods. Using literature data, we did not find complete analogues for the studied clusters in our Galaxy and M31 in terms of age, helium mass fraction (Y), and chemical composition. The alpha-element abundances in four clusters are about 0.2 dex higher than the average for stars in the Galactic field at $[\text{Fe}/\text{H}] \sim -1$ dex. We suggest that these and Maricheva's (Maricheva M. 2021) findings about lower metallicities of the studied objects than the average metallicity of red giants in the M31 halo and about the abundances of alpha-process elements in them corresponding to the average value for stars in the M31 inner halo likely indicate that the star formation process in the vicinity of M31 at the time of our sample clusters formation was complex with the inflow of fresh gas from the intergalactic medium and violent star forming events associated with SNe II bursts.

Keywords: globular clusters: general—globular clusters: individual: Bol6,Bol20, Bol45, Bol50 - galaxies: M31

1 Introduction

The globular cluster (GC) system in the nearest to our Galaxy giant spiral, M31, has been studied in detail in the literature. However, in order to determine ages and metallicities of GCs, their colours and spectral indices were commonly used in comparison with models of stellar populations. For several objects, integrated-light spectroscopic studies were performed in order to determine their chemical composition (Colucci et al. 2014 [hereafter: C14], Sakari et al. 2016 [hereafter: S16], Sharina et al. 2018, Larsen et al. 2018) and age (C14). To date, the deepest colour-magnitude diagrams (CMDs) for clusters in M31 reach confidently the level of the horizontal branch (Federici et al. 2012, Larsen et al. 2021).

In this article, we consider the results of the analysis by Maricheva (2021)(hereafter: MMI21) of integrated-light (hereafter: IL) spectra of four GCs in M31. Our aim is the comparison of the determined ages, helium mass fraction (Y), and the abundances of chemical elements

Fe, C, N, Mg, Ca, and Ti with the corresponding data for Galactic and M31 GCs and with the data for field stars in two galaxies. The comparison of the data for GCs with similar ages and metallicities in different galaxies and different galactic subsystems will ultimately help us to answer the question: how environment and star formation history influence the chemical composition of GCs?

2 Spectroscopic data, methods of their analysis and main results

The spectra of four GCs were obtained in 2020 with the 6-m SAO RAS telescope using the SCORPIO-1 multi-mode focal reducer (Afanasiev et al. 2005) in the long slit mode. The used grism VPHG1200B and the long slit of 1 arcsec provide the resolution FWHM $\sim 5.5 \text{ \AA}$ (full width at half maximum of a single spectral line) within the spectral range 3600-5400 \AA . Please see the paper by

MMI21 describing in detail the observational data and the procedure of their reduction and analysis.

Ages, Y , and the abundances of chemical elements in GCs can be determined using their medium-resolution IL spectra (e.g. Sharina et al. 2020 and references therein). For this, the observed spectra are approximated by the synthetic ones, calculated on the basis of models of stellar atmospheres. The parameters of stellar atmospheres are set by the selected theoretical isochrone of stellar evolution. The synthetic stellar spectra are summed according to the selected stellar mass function. We apply air wavelengths for our analysis¹. The method was tested with the medium-resolution spectra from the Schiavon et al. (2005) library (Sharina et al. 2020). The method is implemented in the program *CLUSTER* (Sharina et al. 2020 and references therein) based on the plane-parallel hydrostatic models of stellar atmospheres calculated with the ATLAS 9 code (Castelli & Kurucz 2003). A proper isochrone is selected by fitting the lines of the Balmer series of hydrogen and CaI 4227, and K, and H CaII 3933.7, and 3968.5 Å lines by the model ones. Following the previous studies, MMI21 applied the stellar mass function by Chabrier (2005) and the scaled-solar isochrones by Bertelli et al. (2008) for the analysis. The chemical composition of the Bertelli et al. (2008) stellar evolutionary models is given relative to the solar abundances of Grevesse & Sauval (1998), in the same abundance scale as the Castelli & Kurucz (2003) models. Additionally, MMI21 used Pietrinferni et al. (2004) isochrones. These models were computed relative to a scaled solar heavy-element distribution from Grevesse & Noels (1993). MMI21 did not find any systematic differences between the chemical abundances derived on the basis of the Bertelli et al. (2008) and Pietrinferni et al. (2004) isochrones.

The abundances of the chemical elements for Bol20, Bol50 were derived by MMI21 for the first time. For all four objects (Bol6, Bol20, Bol45, and Bol50), Y was determined for the first time. All the studied clusters turned out to be older than 10 Gyr with the metallicities in the range: from $-0.75 < [\text{Fe}/\text{H}] < -1.1$ dex²: $T = 11.2 \pm 1$ Gyr, $Y = 0.3 \pm 0.05$, and $[\text{Fe}/\text{H}] = -0.75 \pm 0.1$ dex for Bol 6, $T = 13 \pm 1$ Gyr, $Y = 0.26 \pm 0.01$, and

$[\text{Fe}/\text{H}] = -1.0 \pm 0.1$ dex for Bol 20 and $T = 11 \pm 1$ Gyr, $Y = 0.26 \pm 0.01$, and $[\text{Fe}/\text{H}] = -1.1 \pm 0.1$ dex for Bol 45 and Bol 50. The spectra and the chemical composition of Bol 45 and Bol 50 appeared to be very similar. A reasonable agreement was found between the chemical abundances for Bol6 and Bol45, obtained by MMI21, and the corresponding literature data of high-resolution IL spectroscopy from C14 and S16. The ages of four GCs agree well with the literature ones from C14 and Caldwell et al. (2016).

Fig. 1 demonstrates a comparison between the CMDs of Bol 6 and Bol 45 (Federici et al. 2012), the CMDs of Galactic GCs from Sarajedini et al. (2007), and the evolutionary isochrones by Bertelli et al. (2008) and Pietrinferni et al. (2004) selected by MMI21 for the analysis of the IL spectra of Bol 6 and Bol 45. MMI21 concluded that there are no Galactic GCs in the library of Schiavon et al. (2005) with the spectra very similar to the spectra of four M31 GCs. The Galactic GCs with the CMDs shown in Fig. 1 demonstrate that the spectra are most appropriate for the comparison. In Fig. 2, we illustrate the procedure of spectra fitting. The IL spectrum of Bol 6 analysed by MMI21 is compared with the synthetic one calculated using the isochrone (Fig. 1, panel a) and the chemical composition defined by MMI21 using the method by Sharina et al. (2020). The green line indicates the synthetic spectrum with the decreased abundances of C, N, Ca, and Mg.

3 Comparison of the chemical abundances, determined by Maricheva(2021), with the abundances for GCs and field stars in our Galaxy and M31

In Fig. 3, we compare $[\text{Mg}/\text{Fe}]$, $[\text{Ca}/\text{Fe}]$, and $[\text{Ti}/\text{Fe}]$ abundances for Bol 6, Bol 20, Bol 45, and Bol 50 (MMI21) with the corresponding abundances for GCs in M31 from C14 (red circles). Black points represent the data for Galactic field stars from Venn et al. (2004). In Fig. 4, the same abundances for the Galactic stars are accomplished by the abundances for GCs in M31 from S16 (red circles). Figs. 3 and 4 represent also the abundances of α -process elements from C14 and S16 for the GCs and stars. Alpha-element ratios of GCs were computed by C14 and S16 as follows: $[\alpha/\text{Fe}] = ([\text{Si}/\text{Fe}] + [\text{Ca}/\text{Fe}] + [\text{Ti}/\text{Fe}])/3$. Venn et al. (2004) averaged Mg, Ca, and Ti abundances to cal-

¹ The IAU standard for conversion from air to vacuum wavelengths is given in the study by Morton (1991).

² The abundance of iron in solar units: $[\text{Fe}/\text{H}] = \log(N_{\text{Fe}}/N_{\text{H}}) - \log(N_{\text{Fe}}/N_{\text{H}})_{\odot}$, where $N_{\text{Fe}}/N_{\text{H}}$ is the ratio of the concentrations of iron and hydrogen by the number of atoms or by mass. The mass fractions of hydrogen X , helium Y , and metals Z for the Sun are given by Asplund et al. (2009). $X + Y + Z = 1$.

culate $[\alpha/\text{Fe}]$. MMI21 computed $[\alpha/\text{Fe}]$ as the mean of Mg, Ca, and O abundances. Fig. 5 represents C, N, and O abundances from S16 in comparison with the abundances for our sample four GCs from MMI21. In Fig. 6, we depict the differences in Mg, Ca, Ti, and Mg abundances between the data of S16 and C14 for 19 common objects in these two samples. Note that Figs. 3-5 do not contain the data for Bol6 and Bol45 from C14 and S16 to avoid overlapping symbols. The data for Bol6 and Bol45 from S16 are presented in Fig. 7 together with the abundances for Bol6, Bol20, Bol45, and Bol50 from MMI21 and for Galactic GCs from Sharina et al. (2018) and Sharina et al. (2020), who analysed IL spectra from Schiavon et al. (2005). The data from MMI21 are shown as black dots. The data from S16 for the same GCs are shown as open circles. Green filled squares demonstrate the data for Mayall II in M31 from Sharina et al. (2018). The Galletti et al. (2007) catalogue names of the GCs from C14 and S16 with $-1.1 < [\text{Fe}/\text{H}] < -0.75$ dex are as follows: Bol34, 48, 63, 182, 235, 312, 381, 383, 386 and 403. Their ages estimated by C14 and Caldwell et al. (2016) are older than 10 Gyr. Similar ages were found by MMI21 for Bol 6, Bol 20, Bol 45, and Bol 50. These GCs are located at a distance from the centre of M31 in projection on the sky: $4.4 < R_{\text{M31}} < 7.3$ kpc. The GCs with $-1.1 < [\text{Fe}/\text{H}] < -0.75$ dex from the papers by C14 and S16 are distributed in projection on the sky in the wider high stellar density area around M31. Two of them (excluding two common objects) are pretty close to the GCs from MMI21: Bol 48 and Bol 63. Mg and Ca abundances are high for Bol 63, according to S16: $[\text{Mg}/\text{Fe}] = 0.34 \pm 0.08$, $[\text{Ca}/\text{Fe}] = 0.49 \pm 0.10$.

After the inspection of Figs. 3-7 one can make the following conclusions. (1) The enrichment with the α -process elements is about 0.2 dex higher in four GCs studied by MMI21 than on average in Galactic field stars with $-1.1 < [\text{Fe}/\text{H}] < -0.75$ dex (Venn et al. 2004). (2) The Mg, Ca, and Si abundances for 19 GCs in S16 and C14 agree within the errors (Fig.6). However, the objects in S16 appear to be systematically richer in Ti, especially at low metallicities. (3) We cannot find complete analogues for the studied clusters in our Galaxy and M31 in terms of age, helium content, and chemical composition. The closest analogue for Bol45 is the Galactic GC NGC6637. The chemical composition of Bol 45 (MMI21) and NGC6637 (Sharina et al. 2020) is compared in Fig. 7. The CMDs of the two GCs are compared in Fig. 1. The comparison of their spectra can be seen in Fig. 8. The shallower hydrogen lines in the spectrum of NGC6637 can be explained by the lower helium content. Sharina et al. (2020) selected the following isochrone (Bertelli et al. 2008) to

approximate the spectrum of NGC6637 by the synthetic one: $Z=0.002$, $Y=0.23$ and $T=11.2$ Gyr. These parameters are close to the ones defined by MMI21 for Bol 45, with the exception of Y (Fig. 1, panel c). (4) The chemical abundances of Bol6, Bol20, Bol45, and Bol50 measured by MMI21 agree with that in S16 and C14 (Fig. 7, see also Table 5 in MMI21 for the detailed comparison of the estimated abundances and age with literature values). The most significant exclusion is $[\text{C}/\text{Fe}]$. (5) $[\text{C}/\text{Fe}]$ values of GCs with the metallicities $-1.1 < [\text{Fe}/\text{H}] < -0.75$ dex in S16 are systematically lower than the C abundances of four GCs in MMI21 (Fig. 5). The reason was discussed by S16. The infrared spectral range used by these authors is mainly sensitive to the radiation of bright red giants, characterized by lower $[\text{C}/\text{Fe}]$ than in the case of stars at earlier evolutionary stages. On the other hand, IL spectra in the optical wavelength range are sensitive more to the radiation of Main sequence stars. The systematic shifts between the Ca and Ti abundances at $-1.1 < [\text{Fe}/\text{H}] < -0.75$ dex measured by MMI21, S16, and C14 should be attributed mainly to the differences in the applied methods.

The presence of multiple stellar populations in GCs can reduce Mg and increase helium mass fraction, N and Ca abundances (Carretta & Bragaglia (2021) and references therein). We cannot judge unambiguously about the presence of multiple populations in Bol 6, Bol 20, Bol 45, and Bol 50 using the data from MMI21. MMI21 concluded that the obtained abundances correspond to those in the models of the chemical evolution of the Galaxy under the influence of supernovae type II (SNeII) and hypernovae (Kobayashi et al. 2006) in the metallicity range $[\text{Fe}/\text{H}] = -1.1 \dots -0.75$ dex. MMI21 discovered that the metallicity of four GCs is lower than the average metallicity of red giants in the M31 halo at a given distance from the centre of M31 (Gilbert et al. (2020) and references therein). Using the results of Gilbert et al. (2020), MMI21 concluded that the average abundance of alpha elements in the stars of the inner halo of M31 ($[\alpha/\text{Fe}] = 0.45 \pm 0.09$ dex) is higher than in the stars of the outer halo ($[\alpha/\text{Fe}] = 0.3 \pm 0.16$ dex). The obtained $[\alpha/\text{Fe}]$ values for four GCs correspond to the average $[\alpha/\text{Fe}]$ value for stars in the inner halo at a given distance from the centre of M31.

4 Conclusion

In this article we compared the results of MMI21 on the age, Y, and abundances of Fe, C, N, Mg, Ca and Ti deter-



mination for four GCs in M31 with the available literature data for stars and GCs in two galaxies. We ascertained that four GCs have higher alpha-element abundances at their metallicities than the majority of GCs and field stars in M31 and our Galaxy. MMI21 noted that these alpha-element abundances can be described by the models of the chemical evolution under the influence of SNeII and hypernovae (Kobayashi et al. 2006).

According to MMI21, the obtained abundances of alpha-process elements in four clusters correspond to the average value for stars in the M31 inner halo at a given distance from the centre of M31. The metallicity of the studied clusters is lower than the average metallicity of red giants in the M31 halo (Gilbert et al. 2020). All these facts likely indicate that violent star forming events at the time of the GC formation lead to the high influence of SNeII on their chemical composition. The relatively low metallicities of four GCs can be the indication of the inflows of fresh intergalactic gas.

Further studies of ages and chemical composition of GCs and stars in M31 and its dwarf satellites will help to reveal the origin of GCs and the galactic subsystems they belong to.

5 Acknowledgements

We thank the organizing committee of the annual conference “Modern stellar astronomy” held in Moscow in 2021 in the Sternberg Astronomical Institute for the possibility to discuss these results.

Funding information: The authors state no funding involved.

Author contributions: All authors have accepted responsibility for the entire content of this manuscript and approved its submission.

Conflict of interest: Authors state no conflict of interest.

Data availability statement: The data underlying this article are available in the article.

References

- Afanasiev VL, Moiseev AV. 2005. The SCORPIO universal focal reducer of the 6-m telescope. *Astron. Lett.* 31:194-204. DOI: <https://doi.org/10.1134/1.1883351>.
- Asplund M, Grevesse N, Sauval AJ, Scott P. 2009. The Chemical Composition of the Sun. *Annu. Rev. Astron. Astr.* 47:481-522. DOI: <https://doi.org/10.1146/annurev.astro.46.060407.145222>.
- Bertelli G, Girardi L, Marigo P, Nasi E. 2008. Scaled solar tracks and isochrones in a large region of the Z–Y plane. *Astron. Astrophys.* 484(3):815-830. DOI: <https://doi.org/10.1051/0004-6361/20079165>.
- Caldwell N, Romanowsky AJ. 2016. Star clusters in M31. VII. Global kinematics and metallicity subpopulations of the globular clusters. *Astrophys. J.* 824(1):42. DOI: <https://doi.org/10.3847/0004-637x/824/1/42>
- Carretta E, Bragaglia A. 2021. Excess of Ca (and Sc) produced in globular cluster multiple populations: a first census in 77 Galactic globular clusters. *Astron. Astrophys.* 646:35. DOI: <https://doi.org/10.1051/0004-6361/202039392>.
- Castelli F, Kurucz RL. 2003. New Grids of ATLAS9 Model Atmospheres. In: Piskunov N, Weiss WW, Gray DF. Editors. *IAU Symp. No 210, Modelling of Stellar Atmospheres*. 2002 Jun 17-21; Uppsala, Sweden. IAUS, 2003. p.A20.
- Chabrier G. 2005. The Initial Mass Function 50 years later. In: Corbelli E, Palte F, Zinnecker H, Editors. *The Initial Mass Function: From Salpeter 1955 to 2005*. Dordrecht:Springer. p. 41. DOI: https://doi.org/10.1007/978-1-4020-3407-7_5.
- Colucci JE, Bernstein RA, Cohen JG. 2014. The detailed chemical properties of M31 star clusters. I. Fe, alpha and light elements. *Astrophys. J.* 797(2):116. DOI: <https://doi.org/10.1088/0004-637x/797/2/116>.
- Federici L, Cacciari C, Bellazzini M, Fusi Pecci F, Galletti S, Peirina S. 2012. The horizontal branch luminosity vs. metallicity in M31 globular clusters. *Astron. Astrophys.* 544:13. DOI: <https://doi.org/10.1051/0004-6361/201219317>.
- Galletti S, Bellazzini M, Federici L, Buzzoni A, Fusi Pecci F. 2007. An updated survey of globular clusters in M 31. *Astron. Astrophys.* 471:127-136. DOI: <https://doi.org/10.1051/0004-6361:20077788>.
- Gilbert KM, Wojno J, Kirby EN, Escala I, Beaton RL, Guhathakurta P, Majewski SR. 2020. Elemental Abundances in M31: Iron and Alpha Element Abundances in M31’s Outer Halo. *Astron. J.* 160:41. DOI: <https://doi.org/10.3847/1538-3881/ab9602>.
- Grevesse N, Sauval A. 1998. Standard Solar Composition. *Space Sci. Rev.* 85:161-174. DOI: <https://doi.org/10.1023/A:1005161325181>.
- Grevesse N, Noels A. 1993. Cosmic abundances of the elements. In: Prantzos N, Vangioni-Flam E, Cassé M. Editors. *Symposium in Honour of Hubert Reeves’ 60th birthday: Origin and evolution of the elements*. 1992 Jun 22-25; Paris, France. Cambridge Univ.Press, 1993. p. 15-25.
- Kobayashi C, Umeda H, Nomoto K, Tominaga N, Ohkubo T. 2006. Galactic Chemical Evolution: Carbon through Zinc. *Astrophys. J.* 653(2):1145-1171. DOI: <https://doi.org/10.1086/508914>.
- Larsen SS, Pugliese G, Brodie JP. 2018. Modelling of integrated-light spectra from the optical to the near-infrared: the globular cluster G280 in M31. *Astron. Astrophys.* 617:14. DOI: <https://doi.org/10.1051/0004-6361/201832767>.
- Larsen SS, Romanowsky AJ, Brodie JP. 2021. Hubble Space Telescope imaging of the extremely metal-poor globular cluster EXT8 in Messier 31. *Astron. Astrophys.* 651: A102. DOI: <https://doi.org/10.1051/0004-6361/202141046>.
- Maricheva M. 2021. Study of Integrated Spectra of Four Globular Clusters in M 31. *Astrophys. Bull.* 76:389-404. DOI: <https://doi.org/10.1134/S199034132104009X>.

- Morton DC. 1991. Atomic Data for Resonance Absorption Lines. I. Wavelengths Longward of the Lyman Limit. *Astron. Astrophys. Suppl.* 77:119. DOI: <https://doi.org/10.1086/191601>.
- Pietrinferni A, Cassisi S, Salaris M, Castelli F. 2004. A Large Stellar Evolution Database for Population Synthesis Studies. I. Scaled Solar Models and Isochrones. *Astrophys. J.* 612(1):168. DOI: <https://doi.org/10.1086/422498>.
- Sakari CM, Shetrone MD, Schiavon RP, Bizyaev D, Prieto CL, Beers TC, et al. 2016. Infrared high-resolution integrated light spectral analyses of M31 globular clusters from APOGEE. *Astrophys. J.* 829(2):116. DOI: <https://doi.org/10.3847/0004-637x/829/2/116>.
- Sarajedini A, Bedin LR, Chaboyer B, Dotter A, Siegel M, Anderson J, et al. 2007. The ACS Survey of Galactic Globular Clusters. I. Overview and Clusters without Previous Hubble Space Telescope Photometry. *Astron. J.* 133(4):1658-1672. DOI: <https://doi.org/10.1086/511979>.
- Schiavon RP, Rose JA, Courteau S, MacArthur LA. 2005. A Library of Integrated Spectra of Galactic Globular Clusters. *Astrophys. J. Suppl.* 160(1):163. DOI: <https://doi.org/10.1086/431148>.
- Sharina ME, Shimansky VV, Shimanskaya NN. 2020. Analysis of Integrated-Light Spectra of Galactic Globular Clusters. *Astrophys. Bull.* 75:247-266. DOI: <https://doi.org/10.1134/S1990341320030116>.
- Sharina ME, Shimansky VV, Khamidullina DA. 2018. Age, Helium Content and Chemical Composition of Globular Clusters in the M31 Neighborhood and in our Galaxy. *Astrophys. Bull.* 73:318-334. DOI: <https://doi.org/10.1134/S1990341318030069>.
- Venn KA, Irwin M, Shetrone MD, Tout CA, Hill V, Tolstoy E. 2004. Stellar Chemical Signatures and Hierarchical Galaxy Formation. *Astron. J.* 128(3):1177-1195. DOI: <https://doi.org/10.1086/422734>.

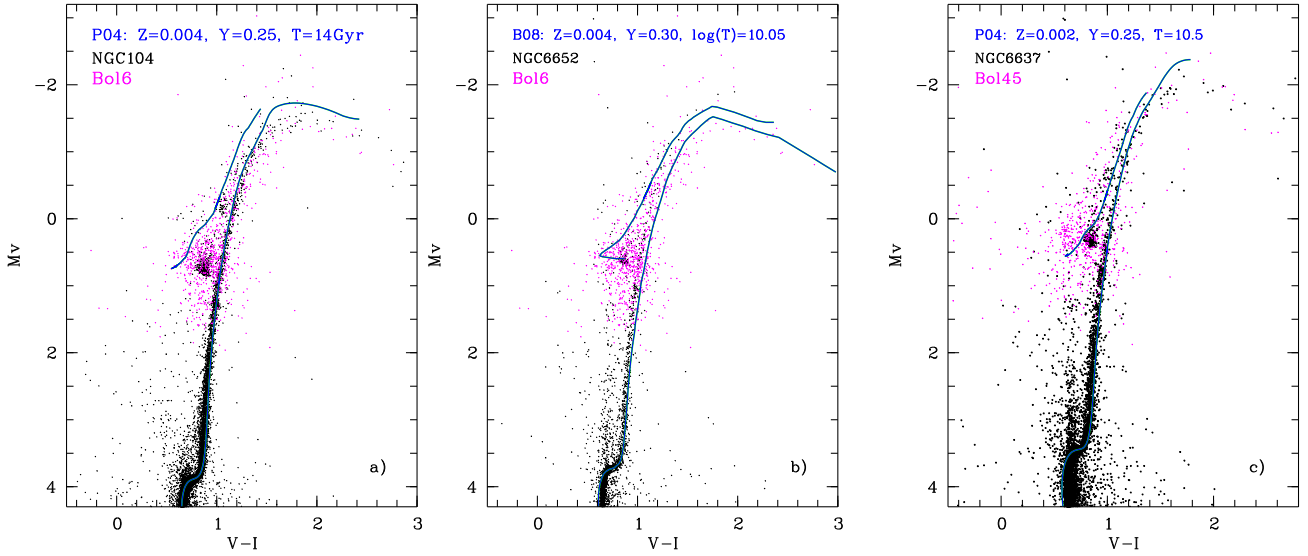


Fig. 1. CMDs for Bol 6 (panels a and b) and Bol 45 (panel c) (Federici et al. 2012) (magenta dots) in comparison with the CMDs of Galactic GCs (Sarajedini et al. 2007) NGC 104, 6652 and 6637 (black dots) and with the evolutionary isochrones (green lines) by Bertelli et al. (2008) for Bol 6 (panel b) and Pietrinferni et al. (2004) for Bol 6 (panel a) and for Bol 45 (panel c), selected by MMI21 for the analysis of the IL spectra of the GCs.

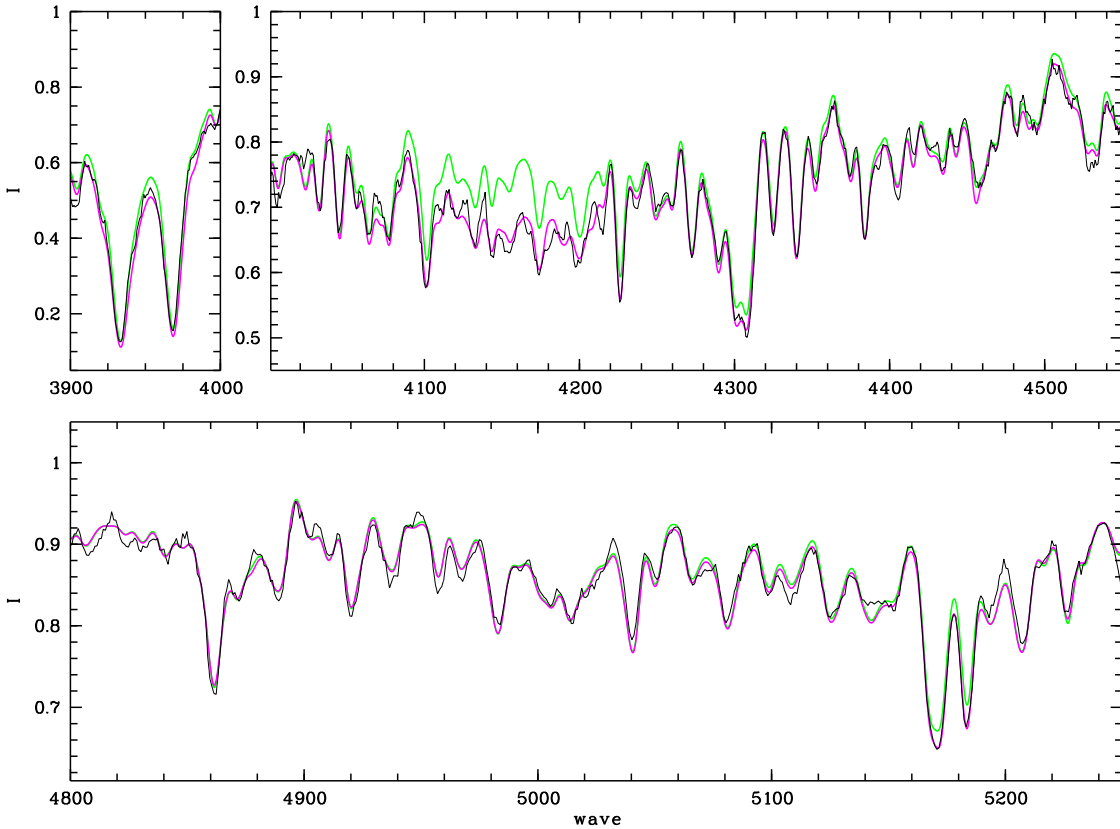


Fig. 2. IL spectrum of Bol 6 from MMI21 (in black) in comparison with the synthetic one calculated using the isochrone from Pietrinferni et al. (2004) (see Fig. 1, panel a) and the chemical composition defined by MMI21 (magenta). A synthetic spectrum with the modified chemical composition is shown in green with Ca, Mg and C depleted by 0.2 dex and N depleted by 0.5 dex.

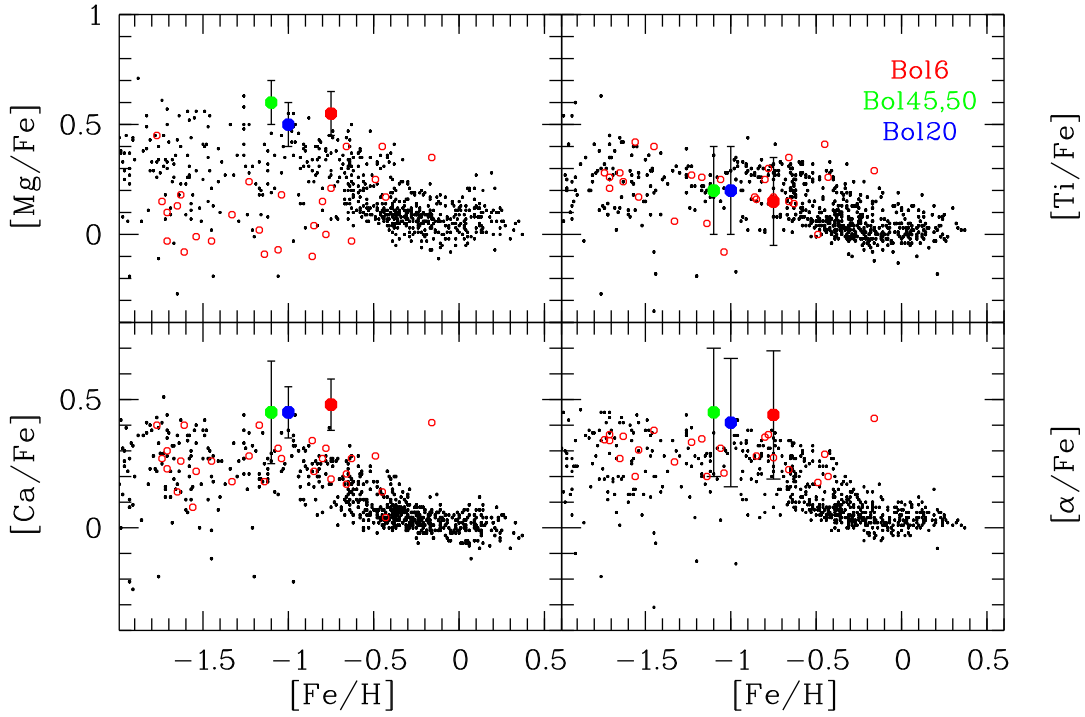


Fig. 3. Ca, Mg and Ti abundances and $[\alpha/\text{Fe}]$ measured by MMI21 for Bol6, Bol20, Bol45, and Bol50 (large filled circles) in comparison with that of Galactic field stars from Venn et al. (2004) (black small dots) and with that of GCs in M31 estimated by C14 (open circles).

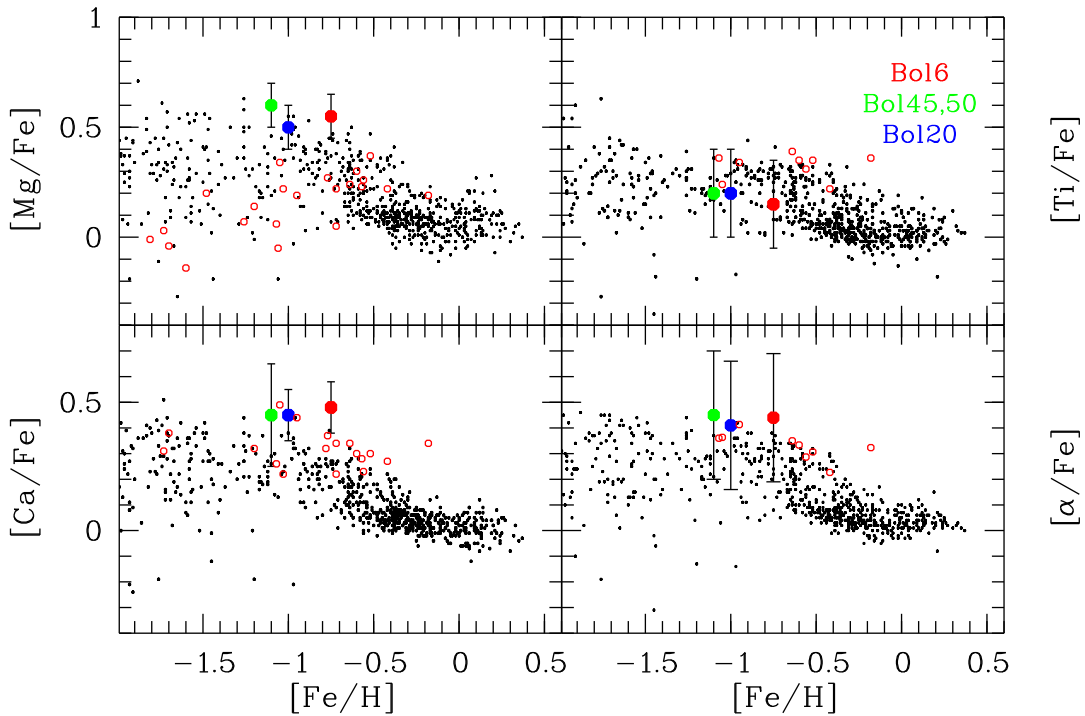


Fig. 4. The same as in Fig.3, but the data for GCs in M31 were determined by S16.

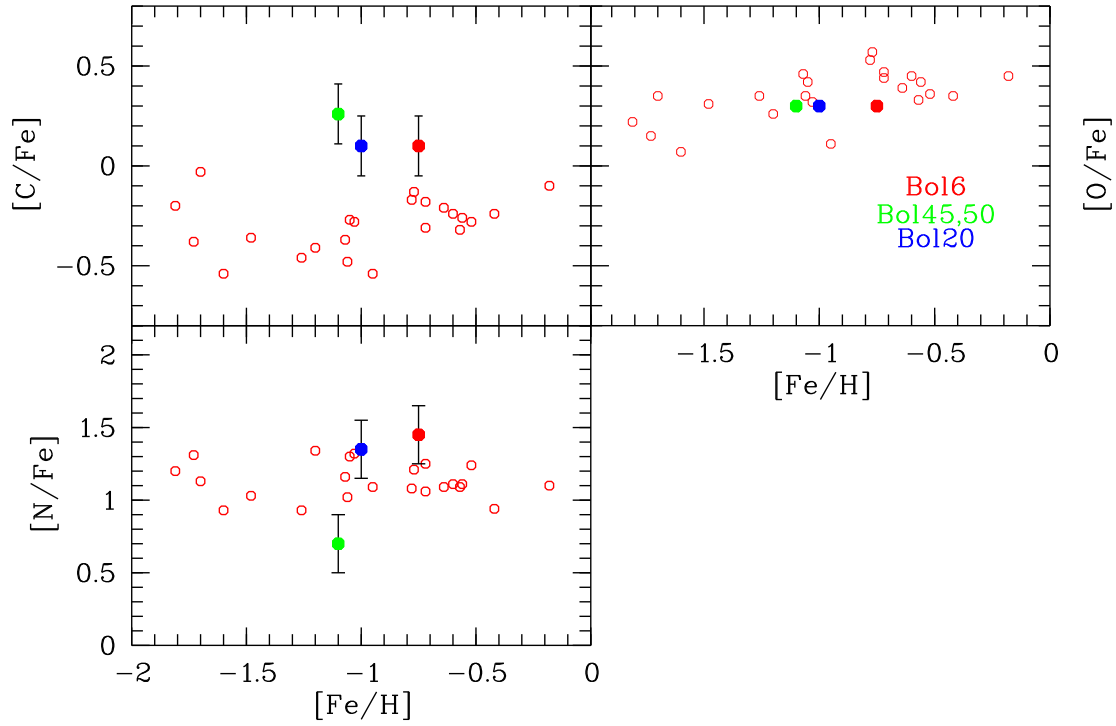


Fig. 5. C, N and O abundances measured by MMI21 for Bol 6, Bol 20, Bol 45, and Bol 50 (filled circles) in comparison with that of GCs in M31 estimated by S16.

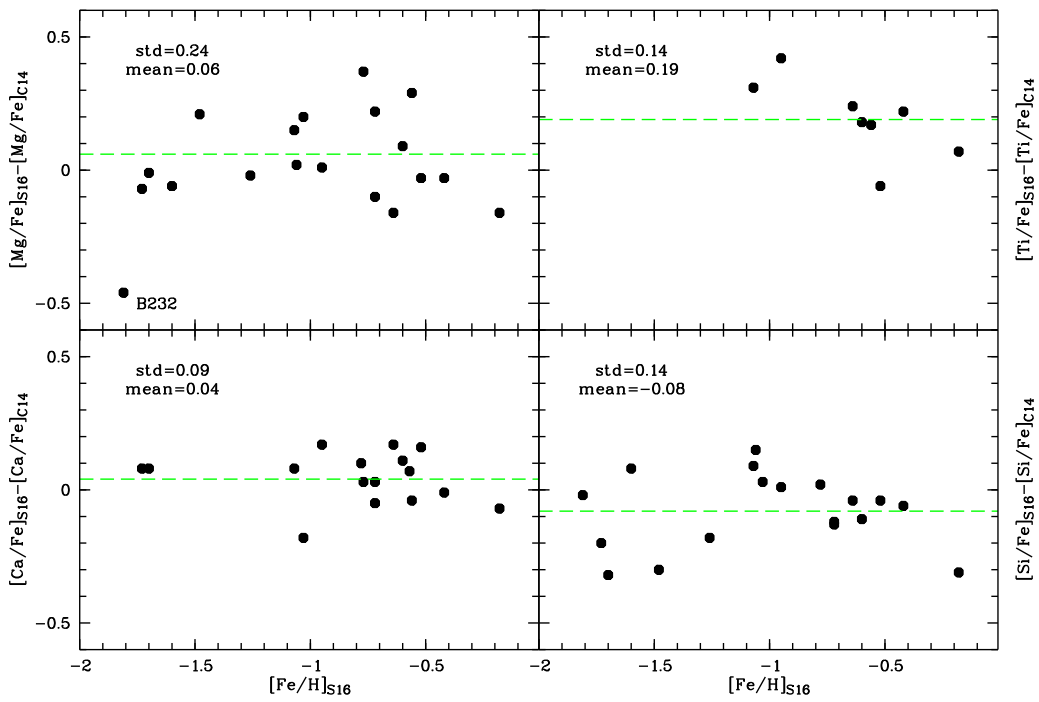


Fig. 6. Comparison between the data from C14 and S16 for 19 common objects.

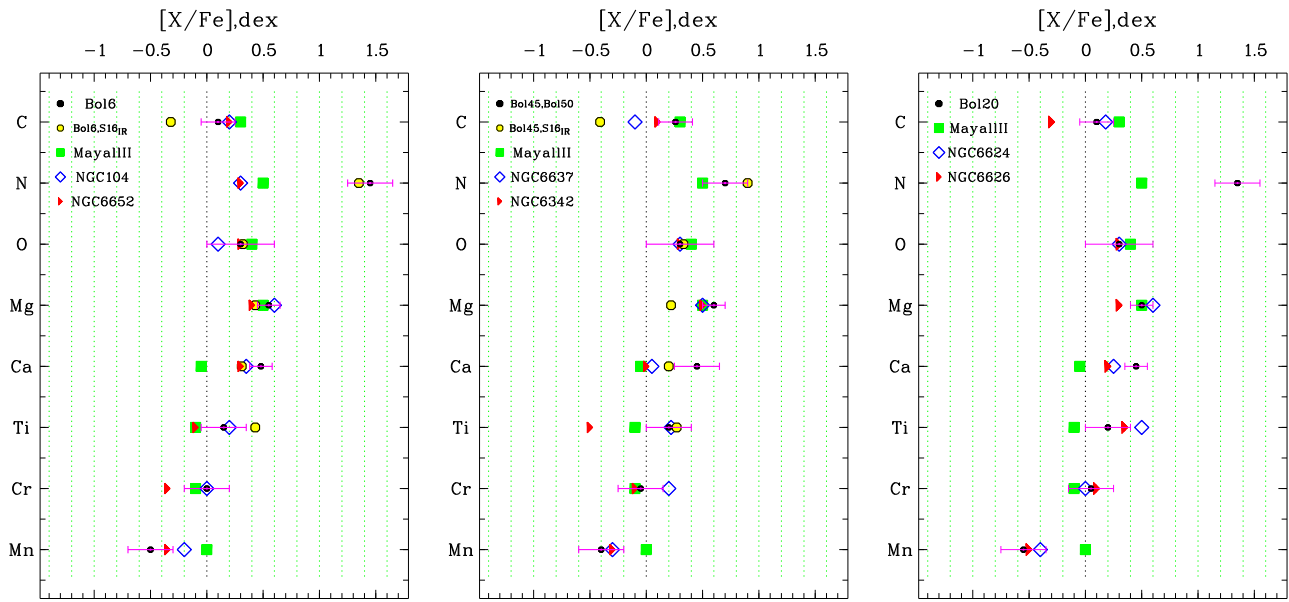


Fig. 7. Abundances of chemical elements determined by MMI21 for Bol 6 (left panel), Bol 45 and Bol 50 (middle panel), and Bol 20 (right panel) using the method of Sharina et al. (2020) (black dots) in comparison with the high-resolution integrated-light spectroscopic abundances from S16 (open circles) and with the abundances for Galactic GCs from Sharina et al. (2018, 2020) (symbols defined in the up left corners of the plots). Note that MMI21 derived the identical abundances for Bol 45 and Bol 50.

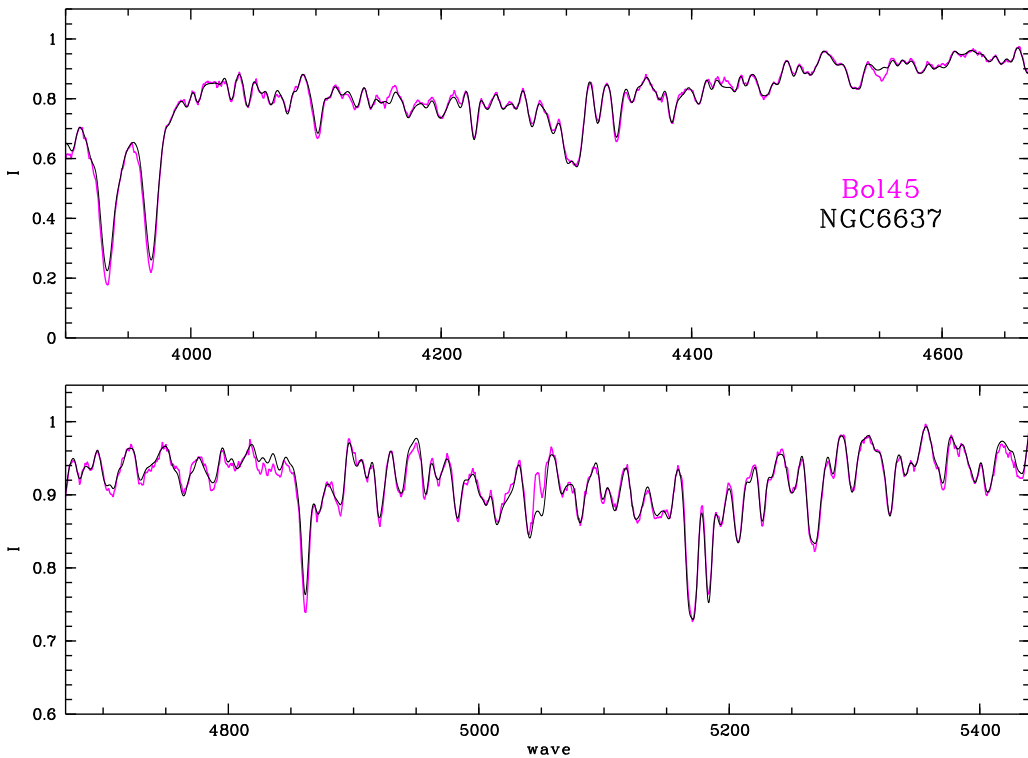


Fig. 8. The IL spectrum of Bol 45 from MMI21 (magenta) in comparison with the spectrum of Galactic GC NGC 6637 (Schiavon et al. 2005) (black).